Microwave Spectrum and Molecular Structure of 3-Fluoro-1,2-epoxypropane and the Unexpected Structure of Its Complex with the Argon Atom

Helen O. Leung,* Mark D. Marshall,* and Devon J. Stuart

Department of Chemistry, Amherst College, P.O. Box 5000, Amherst, MA 01002-5000, United States

Address for correspondence: Prof. Mark D. Marshall
Department of Chemistry
Amherst College
P.O. Box 5000
Amherst, MA 01002-5000
Telephone: (413) 542-2006
Fax: (413) 542-2735
E-mail: mdmarshall@amherst.edu

*Corresponding authors. Fax: +1-413-542-2735; *e-mail addresses:* hleung@amherst.edu (H.O. Leung), mdmarshall@amherst.edu (M.D. Marshall).

The authors declare no competing financial interest.

Abstract

In common with the homologous 3,3-difluoro- and 3,3,3-trifluoro- species, 3-fluoro-1,2-epoxypropane is a small chiral molecule with a simple rotational spectrum, making it potentially useful for chiral analysis via conversion of enantiomers into spectroscopically distinct diastereomers through formation of non-covalently bound complexes. The rotational spectrum of 3-fluoro-1,2-epoxypropane (FO) and of its heterodimer with the argon atom are obtained, along with several isotopologues of each, using Fourier transform microwave spectroscopy from 5.6 to 18.1 GHz, and their structures determined. Surprisingly, the structure of 3-fluoro-1,2-epoxypropane-argon does not show a strong similarity to those previously determined for 3,3-difluoro-1,2-epoxypropane-argon and 3,3,3-trifluoro-1,2-epoxypropane-argon, but rather is more analogous to that of propylene oxide-argon. Equilibrium structural parameters and mapped electrostatic potential surfaces obtained via quantum chemistry calculations are used in rationalizing this result.

I. Introduction

Microwave spectroscopy has recently been demonstrated to be an effective technique for chiral analysis.[1-8] Although enantiomers have the same rotational spectrum, by complexing them with a chiral molecule (a "tag"), they can be converted to spectroscopically distinct diastereomers,[1, 9-10] making it possible to elucidate the absolute configurations of the original enantiomers. Additionally, the rotational transition intensities of the diastereomers can be used to determine enantiomeric excess. Of course, the chiral tagging method depends on the availability of chiral tags, and our group has been actively identifying suitable candidates. So far, we have found two potentially useful tags: 2-(trifluoromethyl)oxirane (TFO)[11] and 2-(difluoromethyl)oxirane (DFO).[12] [These are also known as 3,3,3-trifluoro-1,2-epoxypropane and 3,3-difluoro-1,2-epoxypropane, respectively.] These tags are readily available in enantiopure forms and can be easily introduced into the free-jet expansion. They are small, giving reasonable (*i.e.* large enough) rotational constants for their complexes. Furthermore, they have multiple functional groups – electronegative F and O atoms and electropositive H atoms – to facilitate noncovalent interactions with enantiomeric analytes, yet they do not introduce complicating features, such as internal rotation or nuclear quadrupole hyperfine interactions, into the spectrum. We have already demonstrated that TFO can serve as an effective tag in a self-tagging experiment that forms $(TFO)_2$[13] as well as in distinguishing the two enantiomers of styrene oxide.[14]

Before a tag can be used, its rotational spectrum must first be identified and its structure determined. In this work, we characterize an additional chiral tag candidate, 2-(fluoromethyl)oxirane (FO), also known as 3-fluoro-1,2-epoxypropane or epifluorohydrin. FO is chosen for three reasons. The first is obvious: FO is similar to DFO and TFO except that it has

only one F atom, instead of two and three F atoms, respectively, in the other two tags. Because both DFO and TFO are potentially effective tags, it would be desirable to ascertain if FO is also a good candidate. The second reason is to investigate how the CFH_2 group is positioned in FO. In TFO (Fig. 1a), the three F atoms are arranged to allow for a bifurcated intramolecular interaction between H3 and two F atoms (F_C and F_O) and an interaction between H2 and the third F atom (F_a).[11] In DFO (Fig. 1b), the H atom (H4) in the CF_2H is positioned to interact with the O atom while F_C and F_O still maintain the bifurcated interaction with H3.[12] In the case of FO where the methyl group has only one F atom and two H atoms, it is likely that the group will be arranged to maintain the O···H interaction, but whether the single F atom would take a position similar to F_C or to F_O in TFO or DFO remains an open question.

The third reason for studying FO is to gain a better understanding of why substituted oxiranes bind differently to argon. As a structureless base, argon is useful as a probe of electron density in the oxiranes. In the absence of any substituent, Ar lies in the σ_v plane of oxirane, C_2H_4O, and exhibits a tunneling motion.[15-16] When the symmetry of the oxirane is broken in the presence of a CF_3 or a CF_2H group, Ar binds to TFO[11] and to DFO[12] in a manner similar to that in Ar−C_2H_4O, albeit without any tunneling motion. In these complexes, argon lies on the opposite side of the ring as the substituent. When the substituent is a CH_3 group, however, the binding mode changes. Initially, it was reported that argon does interact with the epoxy ring of propylene oxide, except that it lies on the same side of the ring as the CH_3 group,[17] but subsequent calculations show that the experimental structure is consistent with argon on one edge of the ring, interacting with C and O in the epoxy ring and the C atom in the CH_3 group.[18] Thus, the study of Ar−FO here allows us to fill in the gap: what happens if the methyl substituent

of the oxirane contains only one F atom? Would Ar bind to it in the same manner as it does to TFO and DFO, or would the binding mode be comparable to Ar-propylene oxide?

II. *Ab Initio* Calculations

We use *ab initio* calculations at the MP2/6-311++G(2d,2p) level with GAUSSIAN 16[19] to guide our search for and analyses of the rotational spectra of FO and Ar−FO. To investigate the manner in which the CFH_2 group is positioned relative to the epoxy ring, a scan is carried out where the FCCC dihedral angle is scanned from 0° to 360° in steps of 10° while all other structural parameters are optimized. The potential energy curve shows three minima (Fig. 2), which are then optimized and the corresponding structures are displayed underneath the curve. (The atomic positions in the principal axis system are available as Supporting Information.) The global minimum corresponds to Rotamer (ii), which has an equilibrium energy 68.8 cm^{-1} (0.823 kJ mol^{-1}) and 173.3 cm^{-1} (2.073 kJ mol^{-1}) lower than those of Rotamers (iii) and (i), respectively (Table 1). When harmonic zero-point energy is taken into account, the energy differences between any two rotamers become more pronounced by an additional 7.4 – 18.5 cm^{-1} (0.089 – 0.221 kJ mol^{-1}). It is not surprising that Rotamer (i) has the highest energy. There are two intramolecular interactions: between the F atom and one of the hydrogen atoms bonded to C1 (with an interaction length of 2.447 Å) and between the O atom and an H atom in the methyl group (with an interaction length of 2.812 Å). This configuration, however, places the electronegative O and F atoms only 2.888 Å apart, a distance less than the sum of their van der Waals radii[20] of 2.99 Å and is likely unfavorable. Rotamers (ii) and (iii) both have an intramolecular interaction between an H atom in the methyl group and the O atom (with the same length of 2.601 Å), but Rotamer (ii) places the F atom only 2.669 Å away from the H atom (H3) bound to C2, shorter than the corresponding interaction of 2.724 Å in Rotamer (iii). Even

though it might appear that O in Rotamer (iii) can interact with the second H atom in the methyl group, the interaction length of 2.902 Å is likely too large to give significant stabilization. As a result, Rotamer (ii) is lower in energy. The labeling scheme for Rotamer (ii) is shown in Fig. 2, where the two methyl H atoms are labeled H_a and H_C. The former is almost anti to the H atom of C2 and the latter is on the same side as C1 when the viewed along the C2−C3 bond. The structural parameters for this rotamer are listed in Table 2.

The barrier to interconversion between any two rotamers is greater than 645 cm^{-1} (7.72 kJ mol^{-1}) when equilibrium energies are considered. Specifically, to convert from the global minimum structure to Rotamers (i) and (iii) would take, respectively, 2136 cm^{-1} (25.55 kJ mol^{-1}) and 1018 cm^{-1} (12.18 kJ mol^{-1}). It is, therefore, unlikely that we will observe the higher energy rotamers under our experimental conditions. The rotational constants and dipole moment components of each rotamer are listed in Table 1. The rotational constants of Rotamer (i) are significantly different from the other two rotamers. While this is not the case for Rotamers (ii) and (iii) where their rotational constants differ by no more than 2.4%, the dipole moment components for Rotamer (ii) are much greater. Thus, we expect very strong *b* type transitions, less so for *a* type transitions, and much weaker *c* type transitions for this species. Indeed, the computational results aid us in readily identifying the rotational spectra of several isotopologues of Rotamer (ii) and determining its average structure, as described later.

We use the zero-point average structure (r_0) of FO (given in Section IV) to investigate its interaction potential with argon at the MP2/6-311++G(2d,2p) level using GAUSSIAN 16.[19] The origin of the coordinate system is the center of mass of FO, and the *x*, *y*, and *z* axes are, respectively, the principal *a*, *b*, *c* inertial axes of FO (Figure 3). The position of argon is then specified by its spherical polar coordinates relative to this axis system: *R*, its distance from the

origin; θ, the polar angle formed between *R* and the *z* axis; and ϕ, the azimuthal angle between the *x* axis and the projection of *R* onto the *x*-*y* plane. The value of θ is scanned from 5° to 175° and that of ϕ from 0° to 360°, both in 10° increments, while allowing *R* to optimize. The resulting potential energy contour plot is displayed in Figure 3. Eight minima, labeled (a) – (h), in order of increasing energy are identified and optimized. The structures corresponding to these minima are shown in Figure 4, with the interaction lengths between Ar and each heavy atom listed in Table 3. (The atomic positions for each isomer, in its principal coordinate system, are available as Supporting Information.) The rotational constants, dipole moment components, and relative energies of these structures are listed in Table 4. In addition, we correct for basis set superposition error (BSSE) for these isomers,[21] and the relevant interaction lengths and molecular properties are also listed in Tables 3 and 4. The optimized structures with BSSE correction are similar to those without the correction. In general, the distances between Ar and the heavy atoms are longer by up to 0.24 Å when calculated with BSSE correction than those without the correction. Thus, the rotational constants are typically smaller for the BSSE corrected structures.

As we have done for the minimum energy structures for Ar−DFO[12] and Ar−TFO,[11] we use van der Waals radii of the heavy atoms (Ar: 1.88 Å, C: 1.70 Å, F: 1.47 Å, O: 1.52 Å)[20] to assess the importance of the intermolecular distances in each Ar−FO isomer calculated without BSSE correction. All but two of the heavy distance lengths are longer than the sum of the van der Waals radii of the atoms involved. The two exceptions concern the Ar−O distances in Structures (b) and (g), and they are slightly (only 1%) shorter. Those heavy atom interactions that are less than approximately 10% longer than the sum of the van der Waals radii are indicated in Figure 4. Notably, the lowest energy isomer, Structure (a), is similar to the observed

experimental structures of Ar−DFO[12] and Ar−TFO,[11] where Ar interacts with the heavy atoms on the side of the epoxy ring opposite to the CFH_2 group. Despite extensive searching, however, the rotational spectrum of this species was not identified experimentally. We therefore consider higher level theories, but both MP4 and CCSD with the same basis set as the one we employ for MP2 continue to show that Structure (a) is lower in energy by 10 (0.12 kJ mol^{-1}) and 12 cm^{-1} (0.14 kJ mol^{-1}) than Structure (b), respectively. Even higher levels of theory, such as CCSD(T), are likely needed, but require more resources than available to us. Fortunately, used with caution, the lower levels of theory provide the necessary guidance for our experimental work. Interestingly, density functional calculations with empirical dispersion corrections, such as B3LYP-D3(BJ), which have been successfully applied to larger chiral tagging systems,[22-23] did not provide an increased degree of reliability, although they were admitted much quicker. Inclusion of a harmonic correction to the zero-point energy (calculated at the MP2 level) for each isomer does show a different energy ordering.[24] The corrected energy, E_{zpe}, is reported in Table 4. In addition, we estimate the BSSE correction using this fully relaxed geometry, and also report the energy corrected for both BSSE and zero-point energy in Table 4. With only the zero-point energy correction, Structure (b), an isomer similar to Ar-propylene oxide, becomes the global minimum. Here, Ar lies to one edge of the C2−O bond, interacting with O, C2, and F. Interestingly, the isomer next higher in energy (by 6.8 cm^{-1} or 0.081 kJ mol^{-1}) is Structure (e), where Ar interacts with all three C atoms, followed by Structure (a) at 12.1 cm^{-1} (0.145 kJ mol^{-1}). When both zero-point energy and BSSE are taken into account, the global minimum is Structure (e), and the second highest energy is Structure (b) at 9.5 cm^{-1} (0.114 kJ mol^{-1}). Structure (a) is now higher in energy than Structure (g), where Ar interacts with C1 and O. Our calculation results, therefore, show the difficulties of determining the lowest energy structure, a

consequence of the delicate balance found in intermolecular interactions. Fortunately, with the exception of Structures (b) and (c), the rotational constants and dipole moment components of most of the eight Ar−FO isomers are different enough that we should be able to identify easily the species associated with the observed spectrum. Structures (b) and (c) show Ar interacting with three atoms of the same type (O, F, and C), but with Ar located on the same side of the epoxy ring as the fluoromethyl group in Structure (c) whereas Structure (b) places it on one edge of the C2−O bond.

III. Experiment

The vapor pressure of FO (SynQuest Laboratories) at room temperature is insufficient to be introduced into a sample cylinder for dilution with argon. Instead, 1 atm (absolute) of argon was passed over a sample of the liquid contained in a Swagelok filter body (SS-4TF). The filter element is removed and replaced with glass wool to increase the surface area of the liquid. The filter body was heated briefly with a heat gun until signals appeared. This would introduce sufficient vapor into the system to collect data for 24 – 48 hours.

The 5.6 to 18.1 GHz broadband spectrum is collected using a chirped pulse Fourier transform microwave spectrometer. [25-27] After expanding the gas mixture through two pulsed valves, each with a 0.8 mm diameter nozzle, the sample is polarized using a chirped microwave polarization pulse of 4 μs duration and 20 – 25 W of power. Three separately acquired segments of 4.0 or 4.5 GHz bandwidth are obtained by mixing the output of an arbitrary waveform generator with carrier frequencies of 10.6, 14.6, or 18.6 GHz (generated using phase locked dielectric resonator oscillators) and isolating the lower sideband. The resulting free induction decay (FID) is digitized at 50 Gs s^{-1} for 20 μs beginning 0.5 μs after the end of the excitation pulse. Ten FIDs are collected during each 800 μs opening of the pulsed valves, which operate at 4 Hz. 450,000 to 1,713,000 FIDs are averaged for each segment, and as described previously,[26]

the average is Fourier transformed to give a frequency domain spectrum with a resolution element of 11.92 kHz and typical line widths (FWHM) of 125 kHz. This allows us to assign line centers with an estimated measurement uncertainty of 5 to 10 kHz. We are able to identify readily and assign rotational transitions for five isotopologues of the epoxypropane (the most abundant species, three isotopologues singly substituted with ^{13}C, and one with ^{18}O) and for the most abundant isotopologue of the argon complex in this spectrum. The dynamic range and quality of the chirped pulse signals can be seen from a sample spectrum spanning 200 MHz (Fig. 5). The signals shown are of typical intensity, and this portion contains transitions from all singly substituted ^{13}C and ^{18}O isotopologues of the expoxypropane and the argon complex of the most abundant one.

A more sensitive, higher resolution narrowband Balle-Flygare spectrometer [26, 28] operating in the 5 – 21 GHz range is used to record spectra of the three singly-substituted ^{13}C isotopologues of Ar-FO in natural abundance. The sample was introduced using the same setup as the broadband spectrum, although this instrument has only one pulsed valve and an argon backing pressure of 2 atm was used to enhance complex formation. The background-corrected time domain signals from the Balle-Flygare instrument are digitized for 1024 data points and zero-filled to a 2048-point record length before Fourier transformation to give frequency domain signals with a resolution element of 4.8 kHz. In our experience, line centers in this instrument are determined with a measurement uncertainty estimated to be 2 kHz.

IV. Results

A. Spectral Analysis

1. 3-Fluoro-1,2-epoxypropane

Because the rotational constants of FO are greater than those of DFO, which in turn are greater than those of TFO, we observe fewer rotational transitions for FO. Nevertheless, for the most abundant isotopologue of FO, we have analyzed 58 rotational transitions of all three type (*a*, *b*, and *c* types) with *J* values between 0 and 15 and K_a values between 0 and 4. The *b* type transitions are much more intense than the *a* type, while the *c* type transitions are relatively weak. Qualitatively, these intensities rule out both Rotamer (i) where the *a* type transitions are the weakest and *c* are strongest and Rotamer (iii) where the three dipole moment components are small. They are consistent with those predicted by Rotamer (ii).

In addition to the most abundant isotopologue, we have also observed 14 − 22 rotational transitions due to four additional isotopologues singly substituted with ^{13}C and with ^{18}O in natural abundance, sampling a smaller range of *J* (0 – 8 and 0 – 6, respectively, for the ^{13}C and ^{18}O species) and K_a values (0 – 2 and 0 – 1, respectively, for the ^{13}C and ^{18}O species). Because of the lower abundance of these minor isotopologues, we do not observe any *c* type transitions

The spectrum of each isotopologue is analyzed using the Watson *A*-reduced Hamiltonian[29] and Pickett's nonlinear SPFIT program.[30] The spectroscopic constants are listed in Table 5. The rotational constants are well determined. We are also able to determine 5 quartic and 3 sextic centrifugal distortion constants for the most abundant FO, and 3 – 4 quartic centrifugal distortion constants for the other isotopologues. The rms deviation of each fit is 3 – 5 kHz. Tables of observed and calculated transition frequencies with assignments for all isotopologues studied are provided as Supporting Information.

2. Ar-3-fluoro-1,2-epoxypropane

As indicated earlier, we are unable to observe the rotational spectrum of Structure (a) for Ar-FO. Guided by the similar rotational constants predicted for Structures (b) and (c), we have assigned 105 transitions of all three types (*a*, *b*, and *c*) to the most abundant isotopologue of Ar-FO, over a *J* range of 1 – 10 and a K_a range of 0 – 6. Two *a* type transitions ($5_{23} - 4_{22}$ and $5_{14} - 4_{13}$), marked by diamonds, are shown in Figure 5. They have intensities similar to those of the *b* type transitions for the ^{13}C-containing FO isotopologue. Having similar respective dipole moment components, this suggests that the argon complex is present at levels of roughly 1% in the pulsed jet expansion. We were not able to assign spectra consistent with the predicted rotational constants for other structures.

Only *a* type transitions were obtained for the three isotopologues singly substituted with ^{13}C in natural abundance using the Balle-Flygare spectrometer. These 15 – 16 transitions sample smaller *J* and *K* ranges ($J = 2 - 6$; $K_a = 0 - 2$) than their most abundant counterpart. Nevertheless, as reported later, because the absolute value of the asymmetry parameter for each isotopologue is significantly less than 1, we are able to determine the *A* rotational constants with good precision.

The rotational spectra are again analyzed using the Watson *A*-reduced Hamiltonian[29] and Pickett's nonlinear SPFIT program.[30] The three rotational constants, and five quartic and one sextic centrifugal distortion constants for the most abundant species are listed in Table 6. The rms deviation of the fit for the most abundant species is 4 kHz. For the minor isotopologues, we determine the rotational constants and four quartic centrifugal distortion constants. Because the Balle-Flygare spectrometer has higher resolution, the rms deviation for each of these fits is less

than 0.8 kHz. Tables of observed and calculated transition frequencies with assignments for all isotopologues studied are provided as Supporting Information.

B. Structure Determination

1. 3-Fluoro-1,2-epoxypropane

FO is a near prolate asymmetric top with an asymmetry parameter value between –0.954 and –0.949 for each of the five isotopologues. Although we report the spectroscopic constants using a fit to the Watson *A* reduced Hamiltonian in Table 5, the use of an *S* reduced Hamiltonian yields rotational constants that differ from their *A* reduced counterparts by no more than several kHz; thus, it is immaterial which set of rotational constants are chosen to fit the structure of the molecule. The rotational constants for the ^{13}C and ^{18}O containing isotopologues allow a good determination of the locations of the C and O atoms. Additionally, because the F atom contributes a notable amount to the moment of inertia of the isotopologues, we are able to locate it, too. This is not the case, however, for the H atoms. Thus, all structural parameters involving H atoms are fixed to *ab initio* values. We fit nine parameters to a total of fifteen moments of inertia for the five isotopologues of FO using Kisiel's STRFIT program.[31] For the atoms in the three-membered ring, we fit O−C1, O−C2, and ∠C2−O−C1. (There are only three independent parameters locating these three atoms.) For the heavy atoms outside the ring, we locate C3 by fitting C3−C2, ∠C3−C2−C1, and the C3−C2−C1−O dihedral angle, and F by fitting F−C3, ∠F−C3−C2, and the dihedral angle F−C3−C2−C1. The results of the fit, after converting the parameters to chemically relevant ones using Kisiel's EVAL program,[32-33] are listed in Table 2 and the principal coordinates of the atoms are reported in Table 7. The rms deviation of the fit is 0.0067 u Å^2.

We also determine the Kraitchman substitution coordinates[34] for the C and O atoms in the principal axis system of the most abundant isotopologue of FO from the rotational constants of the four singly substituted species. Although strictly speaking, we can only determine the absolute values of these coordinates, the relative signs of many of them can be assigned based on reasonable chemical distances, and they are listed in Table 7. These substitution coordinates differ from those determined from the structure fit by 0.1 – 4.3%, indicating the vibrational motions of C and O atoms are likely quite harmonic. The greatest difference (11.4%) is between the values for the *c* coordinate of C1. This is because C1 lies practically in the *a*-*b* inertial plane, and the different zero-point motions of the most abundant isotopologue and the one with ^{13}C1 make it difficult to locate the nearly vanishing *c* coordinate in a Kraitchman analysis.

2 Ar-3-Fluoro-1,2-epoxypropane

Ar-FO is an asymmetric top, and all four isotopologues have an asymmetric parameter value between −0.718 and −0.715. The experimental rotational constants of the most abundant isotopologue indicates that the observed species is either Structure (b) or Structure (c). In fact, the experimental values of the *A*, *B*, *C* constants differ from the theoretical value (without BSSE correction) for Structure (b) by 0.8%, 1.4%, and 1.1%, (or 26, 19, and 11 MHz) respectively. These differences are slightly greater with Structure (c); namely, 1.3%, 1.4%, and 1.5% (or 44, 19, and 15 MHz), respectively, again using the theoretical values without BSSE corrections. [Interestingly, the calculated constants with BSSE correction for either structure do not agree as well with the experimental values, differing between 1.9 – 5.4% for Structure (b) and 1.8 – 8.4% for Structure (c).] While the slightly greater difference between the experimental and theoretical rotational constants cannot effectively rule out Structure (c) as the species observed, the rotational constants of the minor isotopologues can.

We locate the three C atoms in the principal axis system of the most abundant isotopologue of Ar-FO using a Kraitchman analysis,[34] and their coordinates are listed in Table 8. They agree very well with those of Structure (b): six of the nine coordinates differ from the theoretical, equilibrium structure by no more than 1.2%. The three coordinates that differ more significantly are those with small magnitude: the *b* coordinate of C2 and the *c* coordinates of C1 and C3, and in these cases, it is more appropriate to consider the absolute differences. These are, respectively, 0.019, 0.006, and 0.036 Å, small enough to be insignificant. The Kraitchman coordinates agree poorly with Structure (c). As a result, we can definitely assign the observed species as Structure (b). In fact, as theoretical calculations show, the zero-point corrected energy of Structure (c) is higher than that of Structure (b) by 17.1 cm^{-1} (20.7 cm^{-1}) without (with) BSSE correction.

Guided by Structure (b) and fixing the structure of FO as determined experimentally in the previous section, the Ar atom is located using Kisiel's STRFIT program.[31] We choose a set of uncorrelated geometric parameters, determined by trial and error, for this purpose – the distance between Ar and C3, the angle formed by Ar, C3, and O, and the dihedral angle formed by Ar, C3, O, and C1 – and fit these quantities to the three moments of inertia of each of the four isotopologues of Ar-FO. The rms deviation of the fit is 0.054 u $Å^2$. The atomic coordinates of each atom are listed in Table 8, and those of the C atoms agree excellently with the corresponding substitution coordinates. Furthermore, the Ar coordinates are similar to those predicted by Structure (b). The heavy atom distances from the structure fit, calculated by Kisiel's EVAL[32-33] program, are listed in Table 3, once again showing their close agreements with those of Structure (b). The experimental structure of the complex is shown in Fig. 6, with the significant interactions labeled.

V. Discussion

The experimental rotational constants of 3-fluoro-1,2-epoxypropane agree remarkably well with the theoretical equilibrium rotational constants of Rotamer (ii): the respective constants differ between 0.2% – 0.8% (or in absolute values, 6 – 118 MHz). Although there are three possible positions for the F atom in the CFH_2 group, as given by the three rotamers in Fig. 2, Rotamers (i) and (iii) are too high in energy to be observed under our expansion conditions. The observed FO molecule has one of the two H atoms (H_a) in the CFH_2 group almost anti to H3: the dihedral angle formed by H_a, C3, C2, and H3 is 173.0(15)°. This configuration allows two intramolecular interactions: $O\cdots H_a$ with a length of 2.602(11) Å and $F\cdots H_3$ at 2.6640(81) Å.

Comparing the structure of FO with those of TFO,[11] DFO,[12] and propylene oxide (PRO)[35] should show the manner in which the epoxy ring structure in ethylene oxide (EO)[36] is affected by the addition of differently substituted methyl groups. As we discovered in our work with DFO, however, it is difficult to draw conclusions regarding the average structures among these species because they exhibit different amounts of vibrational averaging. In fact, the bond lengths between the atoms in the epoxy ring in FO agree to within 3σ with their counterparts in TFO, DFO, PRO, and EO. In other words, the average structure of the epoxy ring in EO appears not to be affected by methyl substitution to a significant extent.

To eliminate vibrational effects, we compare instead the equilibrium structures of the epoxy rings in these species calculated at the MP2/6-311++G(2d,2p) level, which are reported in Table 9. (With the exception of FO, we have reported many of these structural parameters previously.[12]) The two C atoms in the ring are C1 and C2, with C1 connected to two H atoms and C2 connected to a methyl group (if present). First, we consider the effects of F substituents in the methyl group. When there is only one F atom, the epoxy ring differs little from that of

ethylene oxide, but the effects of two or more F atoms in the methyl group are more apparent. We list here the changes of structural parameters for FO, DFO, and TFO, respectively, from the EO values: the C2–O bond lengths decrease by 0.0013, 0.0064, 0.0170 Å, and the C1–O bond lengths increase by 0.0003, 0.0038, 0.0062 Å. The behavior of the C1–C2 bond lengths does not show a regular pattern: FO is longer by 0.0015 Å while those of DFO and TFO are shorter than that of EO by 0.0023 and 0.0028 Å, respectively. Additionally, there is an increase in the C2–C3 bond length as the number of F atoms increases. Taken together, these structural parameters suggest that the difluoromethyl and trifluoromethyl groups tend to increase the electron density in the C2–O and C1–C2 bonds at the expense of the C1–O and C2–C3 bonds and perhaps the H atoms as well. The effects are greater for TFO than DFO. In the case of FO, the C2–O bond has slightly greater electron density than the C1–O bond, likely drawing electron density from it and from the C1–C2 bond. Another indication that the electron densities of C1 and C2 become increasingly different is reflected by the extent that the OC2C1 angle is greater than the OC1C2 angle: 0.11°, 0.69°, and 1.56°, respectively, for FO, DFO, and TFO.

When the methyl group contains no F atom, as in PRO, the C1–C2 bond is essentially the same as that in EO, but both the C1–O and C2–O bonds are longer, by 0.0051 and 0.0031 Å, respectively, than either of the equivalent C–O bonds in EO. It may be that in the presence of the electron donating CH_3 group, the O atom can draw a greater amount of electron density to itself than in EO. It is interesting to note that the C2–C3 bond length in PRO is similar to that in TFO even though the CH_3 group is less bulky than the CF_3 group. suggesting that this length is mostly determined by electrostatic factors in PRO and not steric factors.

In contrast to DFO and TFO, FO forms a complex with argon in an unexpected manner. Despite the fact that the MP2 calculation predicts Structure (a), with a configuration similar to

those found experimentally for Ar-DFO and Ar-TFO, to be the global minimum structure, we do not observe it for Ar-FO. The experimentally observed species for Ar-FO, Structure (b), however, is only 6.6 cm^{-1} (2.3 cm^{-1}) higher in energy without (with) BSSE correction. However, when corrected for harmonic zero-point energy, Structure (b) is the lowest in energy of the eight isomers, but when both BSSE and zero-point corrections are taken into account, Structure (e) is the lowest in energy. Our experimental and computation results, therefore, suggest that we have to exercise caution when searching for the rotational spectrum of a species with isomers that are close in energy. It is remarkable that theoretical methods can guide us so well, but it is unreasonable to expect that they can unequivocally identify the lowest energy species. In fact, although we are only able to observe one species, it is possible that several Ar-FO isomers do exist in the argon expansion (the same applies to Ar-TFO and Ar-DFO).

Ar interacts with three atoms in Ar-EO,[16] Ar-DFO,[12] Ar-TFO,[11] and Ar-FO (Fig. 6). Two of these interactions, Ar–O and Ar–C2, are common to all four species. The third interaction is Ar–F for Ar-FO but is Ar–C1 for the other three. A consideration of the interaction lengths across these species can shed some light onto their strengths. The Ar–O distance, 3.3715(16) Å, is shorter – and thus likely to be stronger – in Ar-FO than those in Ar-EO, Ar-DFO, and Ar-TFO (by 0.077 Å, 0.103 Å, and 0.124 Å, respectively). The Ar–C2 distance in Ar-FO, where the Ar atom is to the side of the ring, 3.7641(17) Å, is comparable to the Ar-C1 distances in Ar-DFO and Ar-TFO (3.758 Å and 3.764(1) Å with the Ar atom above the ring) and much shorter than the 3.8292 Å in Ar-EO. Instead of interacting with another C atom, Ar forms an interaction with F in Ar-FO with a length equal to 3.50757(76) Å. Since an F atom is also present in a similar location in DFO and TFO, it raises the question why Ar does not bind to this F atom in Ar-DFO and Ar-TFO. It is also interesting that although PRO does not have an F atom, Ar-PRO has

structure similar to that of Ar-FO[17-18] (Fig. 6), where Ar forms interactions with C2, O and an H atom.

To explore these questions, we use Gaussian 16 [19] to map the electrostatic potential of the five species, TFO, DFO, FO, EO, and PRO onto their respective total electron density surfaces, both calculated at the MP2/6-311++G(2d,2p) level (Fig. 7). In all cases, it is clear that the O atom is nucleophilic, and the nucleophilicity increases in the order the oxiranes are presented above. (The fact that the O atom in PRO is more negative than that of EO supports the suggestion made earlier that that it draws more electron density from the rest of the molecule in PRO than EO.) It is, therefore, not surprising that Ar interacts with the O atom in all these species. When three F atoms are present in TFO, the only significantly negative portion of the molecule is near O; the F atoms TFO are not particularly nucleophilic. The two F atoms in DFO are somewhat nucleophilic, but the negative potential of the F atom near O and that of the O atom point away from each other, making it sterically impossible for Ar to interact with both. The situation is different in FO: the F atom is very nucleophilic, and it is positioned close enough to O to allow Ar to interact with both. As a result, Ar binds to DFO and TFO differently from FO: through the epoxy ring, just as it does with EO, where the only negative portion of the molecule is the O atom (Fig. 6d).

The binding mode of Ar to PRO is somewhat puzzling because the CH_3 group is not nucleophilic. The Ar−O distance of 3.3299 Å is the shortest of the five complexes shown in Fig. 6 (in accord with the fact that it has the most nucleophilic O atom in the mapped electrostatic potential surfaces in Fig. 7), and the Ar−C2 bond length of 3.7538 Å is comparable to that in Ar-FO and the Ar−C1 distances in Ar-DFO and Ar-TFO. Finally, the Ar−H distance of 3.2123 Å appears to be reasonable. (The Ar−C3 distance of 3.9188 Å in Ar-PRO suggests that this

interaction is weaker than the Ar−C interactions in the fluoromethyl species and may not be too important.) Perhaps by binding off to one side of the C2−O bond, Ar can bind closely to O, and at the same time, minimize unfavorable steric effects that may be present if it were to bind to the epoxy ring.

To attempt to further understand the two different binding modes of Ar, which we term "top" when it binds to the epoxy ring [such as the configuration for Structure (a)] and "side" when it is off to the edge of the C2−O bond [similar to the configuration for Structure (b)], we optimize these two structures for Ar-TFO, Ar-DFO, Ar-FO, and Ar-DFO. Corrections are made for zero-point energy, both harmonically and anharmonically, and for BSSE. The results are listed in Table 10. When we consider only the equilibrium energies, with or without BSSE correction, the top binding mode is always lower in energy than the side binding mode for Ar-TFO, Ar-DFO, and Ar-FO. It is interesting to note that the energy difference between the top and side binding mode is smallest for Ar-FO. When zero-point energy is taken into account, the side binding mode for these species is lower in energy. In fact, the energy difference between these two binding modes is greatest for Ar-FO in most cases. It is therefore not surprising that we observe the side binding mode for Ar-FO; yet we have not observed the same mode for Ar-DFO and Ar-TFO. The computational results also suggest that because the isomers of this type of complexes differ little in energy, one must take great caution in analyzing spectroscopic data and cannot solely rely on computational results. Because we use argon as our buffer gas in our pulsed jet expansion, in which weakly bound complexes are generally believed to undergo repeated formation and dissociation, the observed structures of Ar-FO, Ar-DFO, and Ar-TFO almost certainly represent the lowest energy species. The conformational temperature is expected to be on the order of a few Kelvin, or $kT < 3$ cm^{-1}. It is interesting to note that for Ar-

PRO, theory shows that the side binding mode is lower in energy (equilibrium and zero-point energies, with or without BSSE correction), and in fact, it is indeed the mode observed.

VI. Conclusion

The microwave spectra for five isotopologues of the chiral molecule, 3-fluoro-1,2-epoxypropane (FO), have been observed and assigned. The rotational constants obtained from the analysis of the spectra are used to determine the heavy atom structure of the molecule, with the positions of hydrogen atoms fixed using results from *ab initio* calculations. Only one conformation of the fluoromethyl group is seen in the low effective temperature pulsed jet expansion, consistent with theoretical predictions for the relative energies of the three possibilities. The effect of an increasing degree of methyl group fluorination on the vibrational ground state structural parameters of the epoxy ring in ethylene oxide is complicated by vibrational averaging effects, but equilibrium structures provided by quantum chemistry calculations show systematic trends for the lengths of the two C–O bonds, one increasing in length the other decreasing, in moving from H_2FC– to HF_2C–, and finally F_3C–. The C–C bond length in the ring first lengthens and then shortens along this series. The bond between the ring and methyl carbons is seen to progressively lengthen. These trends are rationalized in terms of the electron withdrawing power of the substituent through comparison with the theoretical equilibrium structure of propylene oxide, which has an electron donating methyl group.

These differences in electron density are also interpreted as contributing to the unexpected, but not unprecedented lowest energy structure of the argon-3-fluoro-1,2-epoxypropane complex. Unlike Ar-TFO[11] and Ar-DFO,[12] which have structures similar to Ar-EO[16] where the argon atom sits above the epoxy ring, argon binds to 3-fluoro-1,2-epoxypropane in a manner similar to that of Ar-propylene oxide.[17-18] In these two species, the argon atom is off

to the side of the ring, interacting with one edge and the methyl (or fluoromethyl) group. Quantum chemistry calculations show very small energy differences between the two possibilities for each of the oxiranes, with the order not consistently agreeing with experiment and sensitive to different zero-point energies in the two geometries. This suggests that the lower energy structure results from a subtle balance between the argon atom seeking regions of high electron density and steric or geometry constraints. Care must be taken in applying the results of theory to these species.

The low vapor pressure of 3-fluoro-1,2-epoxypropane makes it somewhat less attractive as a candidate for chiral analysis via tagging, but otherwise it has suitable characteristics. However, the differences in binding to argon compared to 3,3-difluoro-1,2-epoxypropane and 3,3,3-fluoro-1,2-epoxypropane, species with higher vapor pressures, indicate subtle differences in intermolecular interactions that could be advantageous in particular cases.

Acknowledgements

This material is based on work supported by the National Science Foundation under Grant No. CHE-1856637.

Supporting Information Available: Tables of observed and calculated transition frequencies for five isotopologues of 3-fluoro-1,2-epoxypropane and four isotopologues of the Ar-3-fluoro-1,2-epoxypropane complex that are reported in this study are available as supplementary material, as are the atomic coordinates for the theoretical structures shown in Figures 2 and 4. The complete citation for Gaussian 16 (Ref. 19) is also provided. This material is available free of charge via the Internet at http://pubs.acs.org.

Table 1. Rotational constants, dipole moment components, and relative energies (equilibrium and zero-point corrected)[a] for three rotamers of 3-fluoro-1,2-epoxypropane obtained from *ab initio* calculations at the MP2/6-311++G(2d,2p) level.

	Rotamer (i)	Rotamer (ii)	Rotamer (iii)
A/MHz	10646	14715	14376
B/MHz	3964	3225	3186
C/MHz	3626	2940	2902
$\lvert\mu_a\rvert$ / D	0.025	1.350	0.338
$\lvert\mu_b\rvert$ / D	1.542	3.024	0.492
$\lvert\mu_c\rvert$ / D	2.221	0.324	0.027
E_{equil} / cm^{-1}	173.3	0.0	68.8
E_{zpe} / cm^{-1}	191.8	0.0	79.9

[a]The energy of the most stable rotamer is set to 0.

Table 2. Structural parameters for the global minimum configuration of 3-fluoro-1,2-epoxypropane obtained using *ab initio* calculations at the MP2/6-311++G(2d,2p) level and from a structure fit to the moments of inertia of five isotopologues of the molecule.

	Theory	Experiment[a]
C1−O / Å	1.4425	1.4345(46)
C2−O / Å	1.4409	1.4331(74)
C1−C2 / Å	1.4664	1.4717(53)
C2−C3 / Å	1.4897	1.4940(65)
C3−F / Å	1.3962	1.3972(44)
C3−H_a / Å	1.0866	1.0866
C3−H_C / Å	1.0879	1.0879
C1−H1 / Å	1.0797	1.0797
C1−H2 / Å	1.0812	1.0812
C2−H3 / Å	1.0820	1.0820
∠C1C2O / °	59.486	59.17(26)
∠C2OC1 / °	61.137	61.76(33)
∠OC1C2 / °	59.377	59.07(38)
∠H1C1C2 / °	119.027	119.027
∠H2C1C2 / °	119.215	119.215
∠H3C2C1 / °	118.680	118.680
∠C3C2C1 / °	119.639	119.46(51)
∠FC3C2 / °	109.895	109.57(43)
∠H_aC3C2 / °	110.165	110.165
∠H_CC3C2 / °	110.901	110.901
∠H1C1C2O / °	−103.603	−103.603
∠H2C1C2O / °	103.050	103.050
∠H3C2C1O / °	102.767	102.767
∠C3C2C1O / °	−104.481	−104.62(59)
∠FC3C2C1 / °	152.717	153.61(59)
∠H_aC3C2C1 / °	33.775	33.775
∠H_CC3C2C1 / °	−88.681	−88.681

[a]1σ standard deviations in the parameters are given in parentheses. The parameters without uncertainties are fixed to the *ab initio* values.

Table 3. Interaction lengths between Ar and heavy atoms in eight isomers of Ar-3-fluoro-1,2-epoxypropane obtained from *ab initio* calculations at the MP2/6-311++G(2d,2p) level and from a fit to the experimental moments of inertia of four isotopologues.

	No BSSE Correction	BSSE Correction	No BSSE Correction	BSSE Correction	No BSSE Correction	BSSE Correction	No BSSE Correction	BSSE Correction	
	Structure (a)		Structure (b)		Structure (c)		Structure (d)		
Ar−C1	3.728	3.852	4.652	4.765	4.614	4.759	3.828	3.946	
Ar−C2	3.705	3.846	3.691	3.805	4.174	4.325	4.310	4.464	
Ar−C3	5.141	5.283	4.189	4.348	3.768	3.932	4.146	4.314	
Ar−O	3.485	3.625	3.378	3.518	3.539	3.668	3.543	3.680	
Ar−F	5.481	5.623	3.507	3.670	3.513	3.653	4.834	5.009	
	Structure (e)		Structure (f)		Structure (g)		Structure (h)		Experiment
Ar−C1	3.742	3.744	5.088	5.193	3.590	3.691	5.952	6.072	4.69291(69)
Ar−C2	3.719	3.915	3.880	4.011	4.651	4.771	5.131	5.289	3.7641(17)
Ar−C3	3.972	4.103	3.715	3.866	5.518	5.650	3.639	3.800	4.20186(56)
Ar−O	4.881	4.983	5.216	5.352	3.371	3.497	5.917	6.034	3.3715(16)
Ar−F	5.025	5.264	3.546	3.724	6.303	6.441	3.522	3.703	3.50757(76)

Table 4. Rotational constants, dipole moment components, and relative equilibrium and zero-point corrected energies for eight isomers of Ar-3-fluoro-1,2-epoxypropane obtained from *ab initio* calculations at the MP2/6-311++G(2d,2p) level without and with BSSE correction.

	No BSSE Correction	BSSE Correction	No BSSE Correction	BSSE Correction	No BSSE Correction	BSSE Correction	No BSSE Correction	BSSE Correction
	Structure (a)		Structure (b)		Structure (c)		Structure (d)	
A/MHz	4643	4629	3306	3269	3288	3273	3258	3281
B/MHz	910	861	1334	1244	1296	1205	1118	1038
C/MHz	811	771	992	940	996	939	905	853
$\lvert\mu_a\rvert$ / D	0.150	0.156	3.067	2.965	2.608	2.625	0.055	0.032
$\lvert\mu_b\rvert$ / D	1.944	1.926	0.551	0.670	0.396	0.443	1.535	1.527
$\lvert\mu_c\rvert$ / D	2.548	2.571	1.193	1.340	1.965	1.940	2.817	2.831
$E_{\text{equil}}^{\text{a,b}}$ / cm^{-1}	0.0	0.0	6.6	2.3	19.8	19.4	28.5	16.6
$E_{\text{zpe}}^{\text{a,c}}$ / cm^{-1}	12.1	25.8	0.0	9.5	17.1	30.2	30.9	31.7
	Structure (e)		Structure (f)		Structure (g)		Structure (h)	
A/MHz	3268	3378	4145	4019	7501	7641	6746	6398
B/MHz	1054	979	983	933	719	687	730	697
C/MHz	830	785	853	810	688	660	689	657
$\lvert\mu_a\rvert$ / D	3.125	3.269	0.303	0.403	0.202	0.233	0.196	0.190
$\lvert\mu_b\rvert$ / D	0.587	0.354	2.063	2.075	2.779	2.793	2.527	2.425

$\lvert\mu_c\rvert$ / D	1.029	0.605	2.468	2.457	1.614	1.595	1.998	2.134
E_{equil} / cm^{-1}	29.1	12.5	42.3	32.8	56.0	26.3	110.0	74.5
E_{zpe} / cm^{-1}	6.8	0.0	43.9	47.4	43.5	23.0	96.3	73.3

[a]The energy of the most stable isomer is set to 0 for the structures computed respectively with and without BSSE correction.

[b]The equilibrium energy is determined by using the average, experimental structure of 3-fluoro-1,2-epoxypropane.

[c]A full relaxation of the complex geometry, include the structural parameters of 3-fluoro-1,2-epoxypropane, is used to compute the equilibrium energy (which differ slightly from those where 3-fluoro-1,2-epoxypropane is fixed to its average structure) and the zero-point corrected energy. A counterpoise calculation is then performed using this optimized structure, and the BSSE corrected energy is computed as $E_{zpe} - E_{equil} + E_{BSSE}$.

Table 5. Spectroscopic constants (in MHz, unless otherwise noted) for five isotopologues of 3-fluoro-1,2-epoxypropane.[a,b]

	$CH_2CH(CH_2F)O$	$^{13}CH_2CH(CH_2F)O$	$CH_2{}^{13}CH(CH_2F)O$	$CH_2CH(^{13}CH_2F)O$	$CH_2CH(CH_2F)^{18}O$
A	14832.5371(12)	14730.1763(32)	14724.7473(35)	14660.1647(22)	14249.5918(31)
B	3210.21845(28)	3152.93528(74)	3202.94573(73)	3194.62966(51)	3154.3080(13)
C	2933.92436(26)	2882.17992(59)	2931.44325(67)	2915.85538(42)	2866.35907(82)
Δ_J / 10^{-3}	1.4565(33)	1.384(25)	1.443(23)	1.435(17)	1.436(48)
Δ_{JK} / 10^{-3}	−7.437(29)	−6.49(21)	−7.48(20)	−7.46(14)	−7.37(33)
Δ_K / 10^{-3}	43.39(15)	40.66(53)	44.12(56)	43.52(36)	[43.39][c]
δ_J / 10^{-3}	0.22771(39)	0.2083(23)	0.2216(24)	0.2273(15)	0.2574(77)
No. of rotational transitions	58	22	22	21	14
No. of *a* type	9	6	5	5	5
No. of *b* type	30	16	17	16	9
No. of *c* type	19	0	0	0	0
J range	0 – 15	0 – 8	0 – 8	0 – 8	0 – 6
K_a range	0 – 4	0 – 2	0 – 2	0 – 2	0 – 1
rms/kHz	4.07	5.04	5.38	3.38	4.36

[a]1σ standard deviations in the parameters are given in parentheses.

[b]Additional centrifugal constants are determined for the most abundant isotopologues: δ_K = 3.630(38) kHz, Φ_J = 0.116(13) Hz, Φ_{KJ} = 23.6(27) Hz, and Φ_K = −105(15) Hz, and are fixed at these values for the 4 minor isotopologues.

[c]Fixed at the value appropriate to the most abundant isotopologue.

Table 6. Spectroscopic constants (in MHz, unless otherwise noted) for four isotopologues of the Ar-3-fluoro-1,2-epoxypropane complex.[a]

	Ar−$CH_2CH(CH_2F)O$	Ar−$^{13}CH_2CH(CH_2F)O$	Ar−$CH_2{}^{13}CH(CH_2F)O$	Ar−$CH_2CH(^{13}CH_2F)O$
A	3331.50027(43)	3291.6875(34)	3325.1426(26)	3304.4252(45)
B	1315.05556(17)	1299.06497(25)	1308.38959(17)	1306.34093(34)
C	980.84334(15)	968.53748(17)	977.49241(12)	973.68185(24)
Δ_J / 10^{-3}	3.9072(17)	3.7655(24)	3.8656(17)	3.8366(32)
Δ_{JK} / 10^{-3}	26.637(14)	25.118(19)	26.275(13)	26.538(26)
Δ_K / 10^{-3}	−11.556(24)	−11.556[b]	−11.556[b]	−11.556[b]
δ_J / 10^{-3}	1.00224(58)	0.9705(13)	0.98822(88)	0.9847(17)
δ_K / 10^{-3}	19.048(11)	18.041(62)	18.798(44)	18.923(84)
Φ_{KJ} / 10^{-6}	−3.31(50)	−[3.31][b]	−[3.31][b]	−[3.31][b]
No. of rotational transitions	105	16	15	16
No. of *a* type	48	16	15	16
No. of *b* type	18	0	0	0
No. of *c* type	39	0	0	0
J range	1 – 10	2 – 6	2 – 6	2 – 6
K_a range	0 – 6	0 – 2	0 – 2	0 – 2
rms/kHz	4.47	0.57	0.39	0.78

[a]1σ standard deviations in the parameters are given in parentheses.

[b]Fixed at the value appropriate to the most abundant isotopologue.

Table 7. Coordinates of the atoms in 3-fluoro-1,2-epoxypropane determined from a structure fit of five isotopologues and the substitution coordinates for four atoms from a Kraitchman analysis.[a]

	a / Å	*b* / Å	*c* / Å
(i) From structure fit			
C1	−1.7001(15)	−0.4929(45)	−0.0431(73)
C2	−0.3736(37)	−0.1376(92)	0.4860(40)
C3	0.8521(40)	−0.6002(28)	−0.2322(65)
O	−1.1766(13)	0.8339(17)	−0.1961(50)
F	1.9071(21)	0.2777(27)	0.0295(46)
H_a	0.6715(75)	−0.625(15)	−1.3034(63)
H_C	1.1627(60)	−1.5808(63)	0.122(15)
H1	−2.5301(41)	−0.5835(76)	0.642(12)
H2	−1.7675(82)	−1.063(12)	−0.959(12)
H3	−0.2681(80)	0.037(19)	1.5486(55)
(ii) Substitution coordinates[b]			
C1	−1.69719(88)	−0.4922(31)	−0.048(31)
C2	−0.3577(42)	−0.137(11)	0.4830(31)
C3	0.8498(18)	−0.5951(25)	−0.2295(65)
O	−1.1754(13)	0.8332(18)	−0.1878(80)

[a]Costain errors[37] (0.0015 $Å^2/z$) in the parameters are given in parentheses.

[b]Although only the absolute values of the substitution coordinates can be determined from the Kraitchman analysis, the relative signs are assigned using physically reasonable atomic distances. The *c* coordinate of C1 is not well determined; its sign is set to be the same as those from the structure fit.

Table 8. Coordinates of the atoms in Ar-3-fluoro-1,2-epoxypropane determined from a structure fit of four isotopologues and the substitution coordinates for the carbon atoms from a Kraitchman analysis.[a] The coordinates of the six heavy atoms in the complex for Structures (b) and (c) calculated at the MP2/6-311++(2p,2d) level (without BSSE correction) are also presented.

	a / Å	*b* / Å	*c* / Å
(i) From structure fit			
C1	−2.18919(68)	−1.37227(66)	−0.0627(17)
C2	−1.3716(17)	−0.22716(44)	−0.49419(6)
C3	−1.61418(54)	1.11785(43)	0.1092(20)
O	−0.8335(16)	−1.22497(35)	0.3825(28)
F	−0.44092(89)	1.87444(20)	0.0530(13)
H_a	−1.9173(37)	1.0135(13)	1.1474(29)
H_C	−2.3690(20)	1.66455(74)	−0.4520(51)
H1	−2.3604(24)	−2.18381(84)	−0.7541(15)
H2	−2.9372(27)	−1.2274(14)	0.7043(43)
H3	−0.9512(50)	−0.2356(14)	−1.4912(15)
Ar	2.36285(10)	−0.23179(39)	−0.02250(33)
(ii) Substitution coordinates[b]			
C1	−2.16995(69)	−1.3683(11)	−0.098(15)
C2	−1.3133(11)	−0.2230(67)	−0.4933(30)
C3	−1.59844(94)	1.1201(13)	0.093(16)
(iii) Structure (b) from MP2 calculation			
C1	−2.1580	−1.3857	−0.1044
C2	−1.3157	−0.2424	−0.4907
C3	−1.6210	1.1136	0.0570
O	−0.8474	−1.2141	0.4529
F	−0.4536	1.8808	0.0846
Ar	2.3465	−0.2273	−0.0307
(iv) Structure (c) from MP2 calculation			
C1	−2.1435	−1.2937	0.3948

C2	−1.7998	−0.0117	−0.2408
C3	−1.1215	1.0489	0.5636
O	−1.0314	−1.1921	−0.5055
F	−0.3739	1.8718	−0.2826
Ar	2.3527	−0.3181	0.0524

[a]Costain errors[37] (0.0015 Å^2/z) in the parameters are given in parentheses.

[b]Although only the absolute values of the substitution coordinates can be determined from the Kraitchman analysis, the relative signs are assigned using physically reasonable atomic distances.

Table 9. A*b initio* equilibrium bond lengths calculated at the MP2/6-311++G(2d,2p) level for the epoxy ring for ethylene oxide and four additional epoxypropanes.[a]

	Ethylene oxide	Propylene oxide	3-Fluoro-1,2-epoxypropane	3,3-Difluoro-1,2-epoxypropane	3,3,3-Trifluoro-1,2-epoxypropane
C1−O / Å	1.4422	1.4473	1.4425	1.4460	1.4484
C2−O / Å	1.4422	1.4453	1.4409	1.4358	1.4252
C1−C2 / Å	1.4649	1.4653	1.4664	1.4626	1.4621
C2−C3 / Å	--	1.4987	1.4897	1.4919	1.4990
∠OC2C1 / °	59.48	59.63	59.49	59.85	60.20
∠OC1C2 / °	59.48	59.50	59.38	59.16	58.64

[a]C1, C2, and O form the epoxy ring, and C3 is the methyl carbon bonded to C2.

Table 10. Relative equilibrium and zero-point corrected energies (in cm $^{-1}$) for two isomers each of four argon complexes obtained from *ab initio* calculations at the MP2/6-311++G(2d,2p) level without and with BSSE correction.[a,b]

	No BSSE Correction	BSSE Correction	No BSSE Correction	BSSE Correction	No BSSE Correction	BSSE Correction	No BSSE Correction	BSSE Correction
	Ar-TFO		Ar-DFO		Ar-FO		Ar-PRO	
E_{MP2}, top	0	0	0	0	0	0	18.6	21.1
E_{MP2}, side	15.0	9.6	16.4	9.2	7.1	2.9	0	0
$E_{zpe,harm}$ top	0.7	6.0	1.8	9.0	12.1	16.3	27.7	30.2
$E_{zpe,harm}$ side	0	0	0	0	0	0	0	0
$E_{zpe,anharm}$ top	0.6	6.0	4.6	11.9	7.7	11.8	27.6	30.1
$E_{zpe,anharm}$ side	0	0	0	0	0	0	0	0

[a]The energy of the more stable isomer for each species is set to 0 for the two structures (top or side) computed respectively with and without BSSE correction.

[b]A full relaxation of the complex geometry, include the structural parameters of each oxirane, is used to compute the equilibrium energy (E_{MP2}) and the zero-point (harmonic or anharmonic) corrected energy**.** A counterpoise calculation is then performed using this optimized structure**,** and the BSSE corrected energy is computed as $E_{zpe} - E_{equil} + E_{BSSE}$.

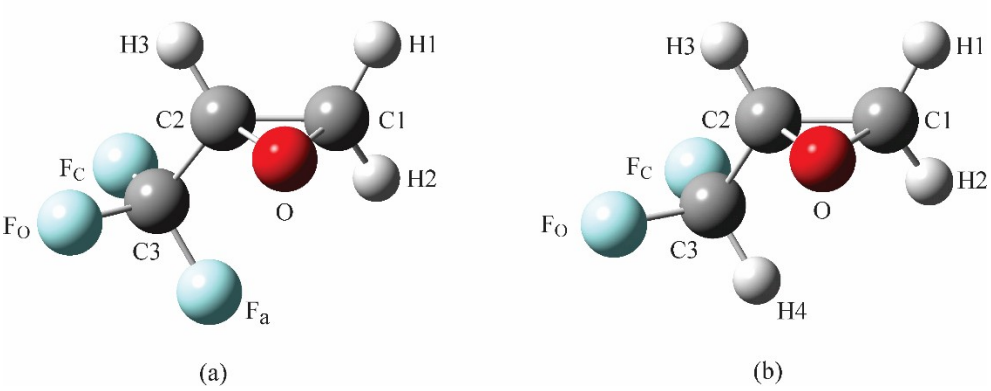

Figure 1. Structures of (a) 2-(trifluoromethyl)oxirane, TFO and (b) 2-(difluoromethyl)oxirane, DFO. Atom colors: C, dark gray; H, light gray; O, red; F, light blue.

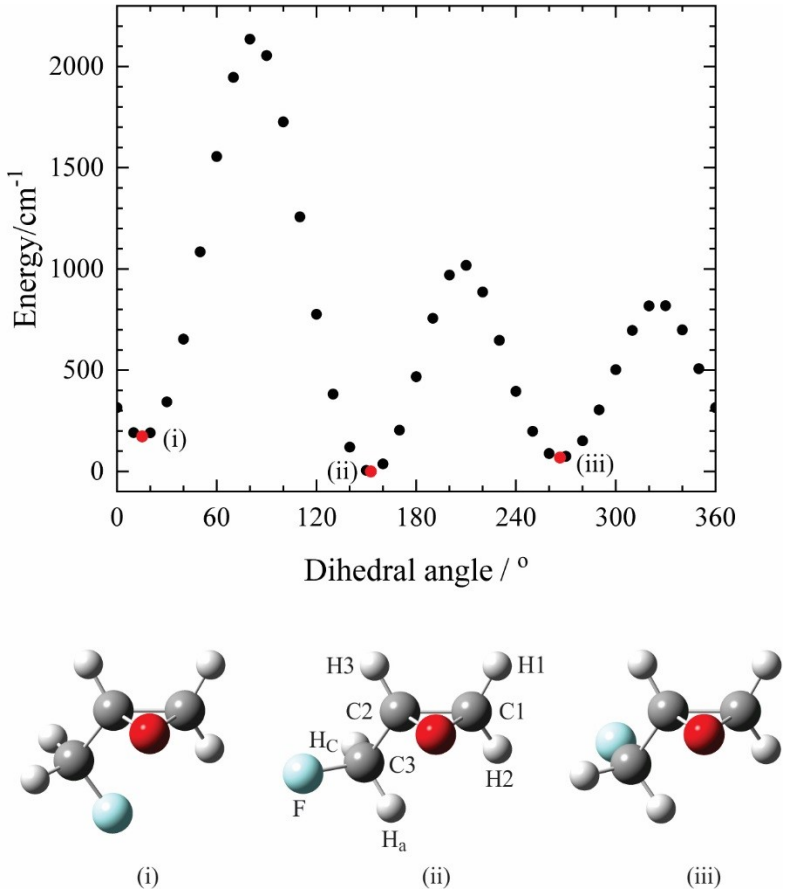

Figure 2. Relaxed scan of the dihedral angle formed by the F atom with C3, C2, and C1 in 3-fluoro-1,2-epoxypropane from 0º to 360º in steps of 10º. The minima are optimized and displayed in red, with the corresponding structures underneath. The labeling scheme for the atoms in the global minimum structure is also shown. Atom colors: C, dark gray; H, light gray; O, red; F, light blue.

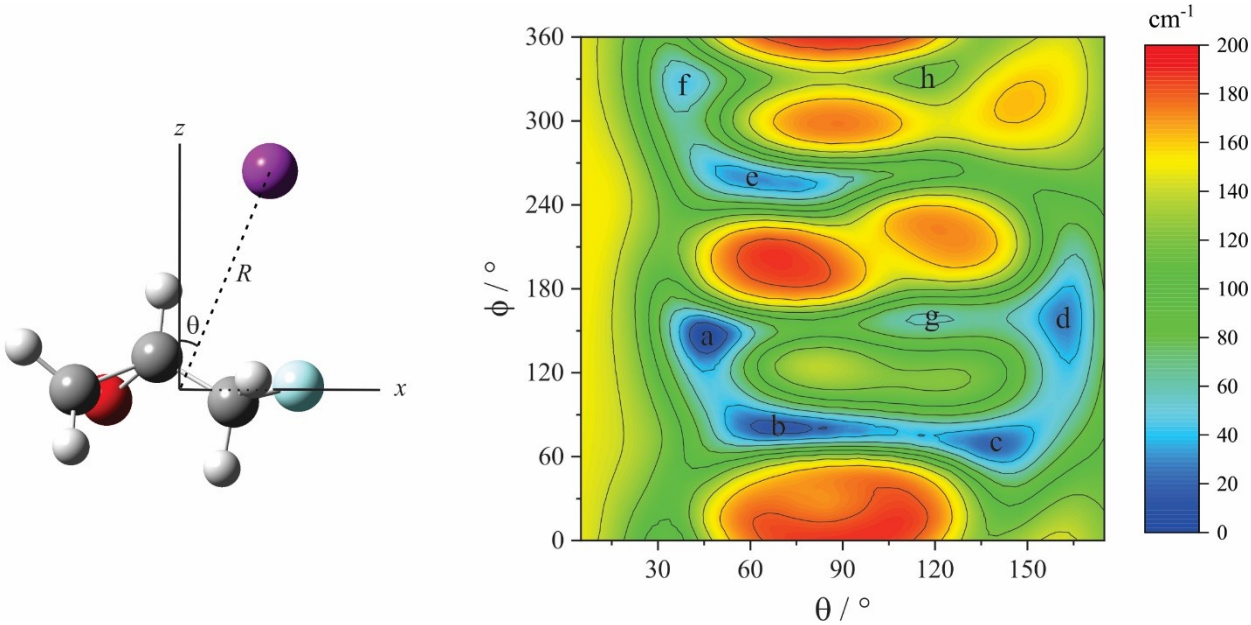

Figure 3. Left: spherical polar coordinate system used to locate Ar with respect to 3-fluoro-1,2-epoxypropane. The *x*, *y*, and *z* axes are the *a*, *b*, and *c* axes for the propane, with the origin at its center of mass. (The *y* axis is directed into the plane of the figure.) *R* is the distance between Ar and the origin, and θ and ϕ (not shown) are, respectively, the polar and azimuthal angles formed by *R* and the coordinate system. Right: contour plot of the potential energy as a function of the angles with *R* optimized. Eight minima are located, and the geometry is optimized at each. The corresponding structures are shown in Figure 4. Atom colors: C, dark gray; H, light gray; O, red; F, light blue; Ar, purple.

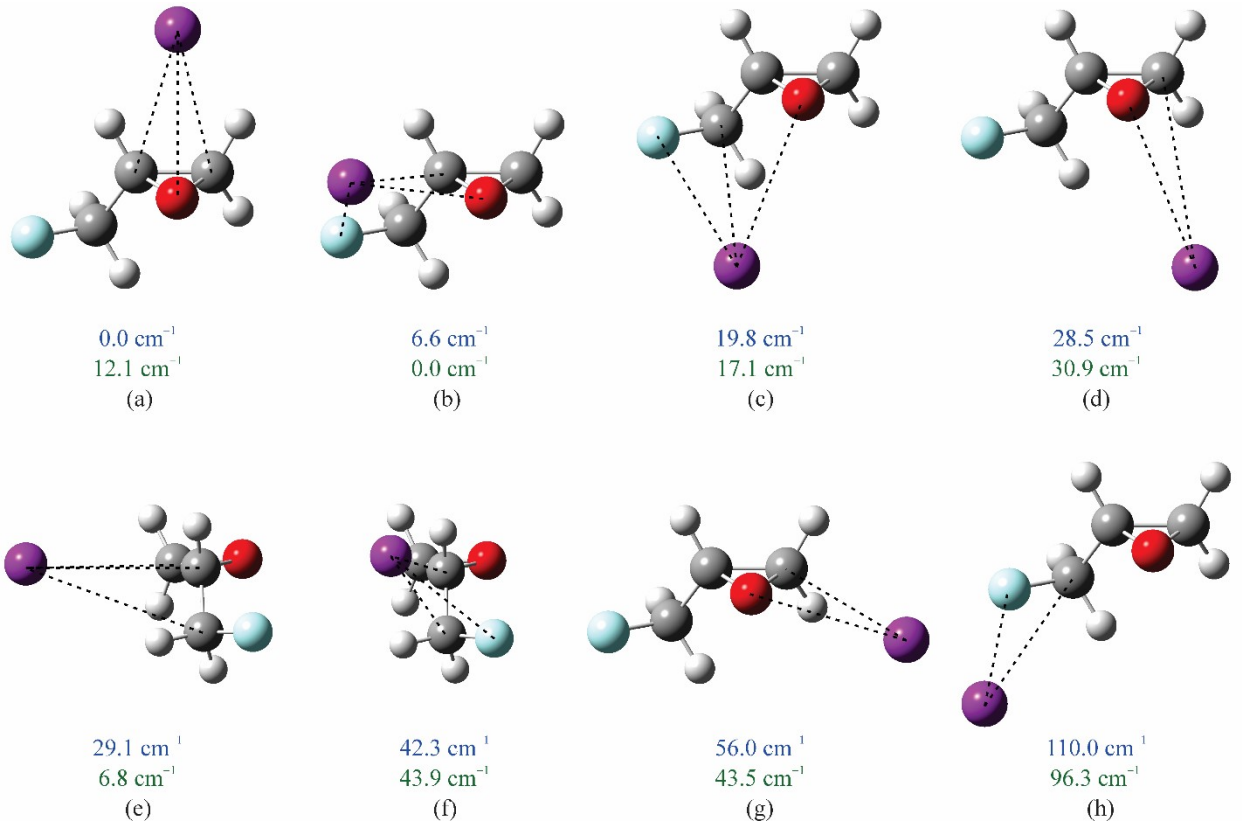

Figure 4. Optimized structures (without BSSE correction) corresponding to the eight minima found in the potential scan for Ar-3-fluoro-1,2-epoxypropane. The more important intermolecular interactions are indicated using dashed lines. Atom colors: C, dark gray; H, light gray; O, red; F, light blue; Ar, purple. The equilibrium and (harmonic) zero-point corrected energies are in blue and green, respectively, both without BSSE correction.

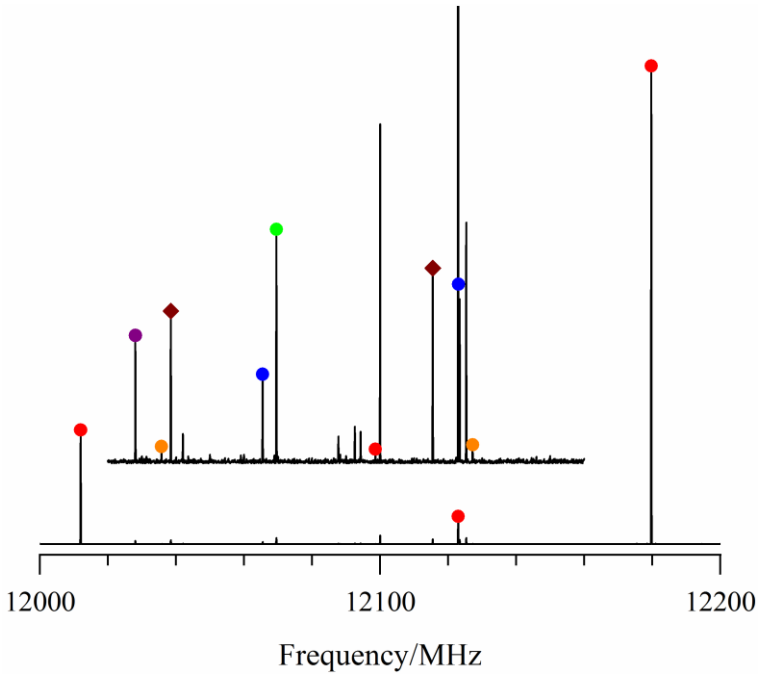

Figure 5. 200 MHz segment of the chirped pulse spectrum taken with 3-fluoro-1,2-epoxypropane in Ar. The bottom trace shows a few strong lines, which, when magnified by 20x, shows the weaker signals. The lines marked by red, blue, green, purple, and orange circles, respectively, are due to the most abundant species of 3-fluoro-1,2-epoxypropane, and its isotopologues substituted with ^{13}C in the C1, C2, C3 positions and that substituted with ^{18}O. The lines marked in brown diamonds are due to Ar-3-fluoro-1,2-epoxypropane.

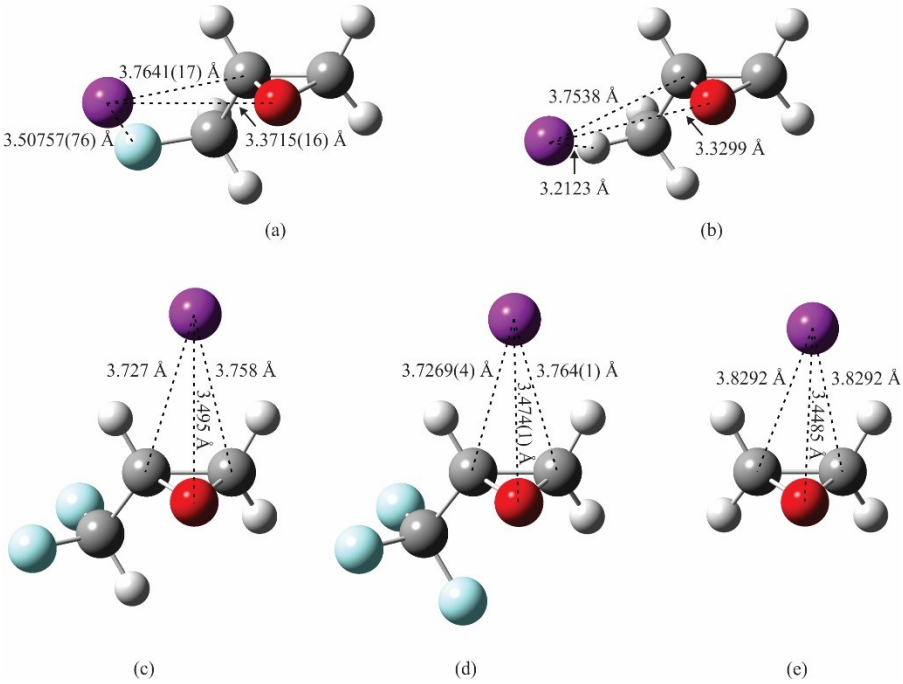

Figure 6. (a) Experimental structure of Ar-3-fluoro-1,2-epoxypropane; (b) Structure of Ar-propylene oxide consistent with the rotational constants reported in references 17 and 18; Experimental structures of (c) Ar-3,3-difluoro-1,2-epoxypropane,[11] (d) Ar-3,3,3-trifluoro-1,2-epoxypropane,[12] and (e) Ar-ethylene oxide.[16] Atom colors: C, dark gray; H, light gray; O, red; F, light blue; Ar, purple.

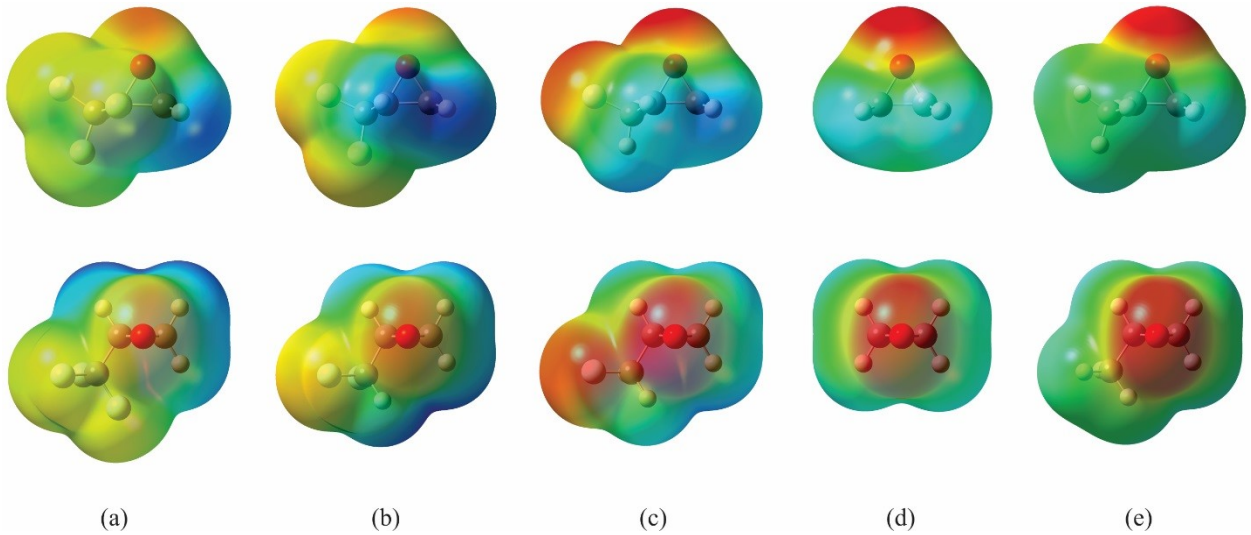

Figure 7. Electrostatic potential, mapped onto a total electron density isosurface for (a) 3,3,3-trifluoro-1,2-epoxypropane, (b) 3,3-difluoro-1,2-epoxypropane, (c) 3-fluoro-1,2-epoxypropane, (d) ethylene oxide, and (e) propylene oxide. Each is shown in two views. The same value of electron density is used for the isosurface in all molecules and identical color scales are used. Blue color represents positive electrostatic potential and red, negative electrostatic potential.

References

1. Evangelisti, L.; Caminati, W.; Patterson, D.; Thomas, J.; Xu, Y.; West, C.; Pate, B. A Chiral Tagging Strategy for Determining Absolute Configuration and Enantiomeric Excess by Molecular Rotational Spectroscopy. The 72nd International Symposium on Molecular Spectroscopy, Talk RG-03, Urbana-Champaign, IL, 2017.
2. Patterson, D.; Schnell, M. New Studies on Molecular Chirality in the Gas Phase: Enantiomer Differentiation and Determination of Enantiomeric Excess. *Phys. Chem. Chem. Phys.* **2014,** *16*, 11114-11123.
3. Shubert, V. A.; Schmitz, D.; Pérez, C.; Medcraft, C.; Krin, A.; Domingos, S. R.; Patterson, D.; Schnell, M. Chiral Analysis Using Broadband Rotational Spectroscopy. *J. Phys. Chem. Lett.* **2016,** *7*, 341-350.
4. Patterson, D.; Schnell, M.; Doyle, J. M. Enantiomer-Specific Detection of Chiral Molecules Via Microwave Spectroscopy. *Nature* **2013,** *497*, 475-477.
5. Patterson, D.; Doyle, J. M. Sensitive Chiral Analysis Via Microwave Three-Wave Mixing. *Phys. Rev. Lett.* **2013,** *111*, 023008.
6. Shubert, V. A.; Schmitz, D.; Patterson, D.; Doyle, J. M.; Schnell, M. Identifying Enantiomers in Mixtures of Chiral Molecules with Broadband Microwave Spectroscopy. *Angew. Chem. Int. Ed.* **2014,** *53*, 1152-1155.
7. Shubert, V. A.; Schmitz, D.; Medcraft, C.; Krin, A.; Patterson, D.; Doyle, J. M.; Schnell, M. Rotational Spectroscopy and Three-Wave Mixing of 4-Carvomethanol: A Technical Guide to Measuring Chirality in the Microwave Region. *J. Chem. Phys.* **2015,** *142*, 214201.

8. Shubert, V. A.; Schmitz, D.; Schnell, M. Enantiomer-Sensitive Spectroscopy and Mixture Analysis of Chiral Molecules Containing Two Stereogenic Centers – Microwave Three-Wave Mixing of Menthone. *J. Mol. Spectrosc.* **2014,** *300*, 31-36.

9. Borho, N.; Xu, Y. Lock-and-Key Principle on a Microscopic Scale: The Case of the Propylene Oxide···Ethanol Complex. *Angew. Chem. Int. Ed.* **2007,** *46*, 2276-2279.

10. Seifert, N. A.; Pérez, C.; Neill, J. L.; Pate, B. H.; Vallejo-López, M.; Lesarri, A.; Cocinero, E. J.; Castaño, F. Chiral Recognition and Atropisomerism in the Sevoflurane Dimer. *Phys. Chem. Chem. Phys.* **2015,** *17*, 18282-18287.

11. Marshall, M. D.; Leung, H. O.; Wang, K.; Acha, M. D. Microwave Spectrum and Molecular Structure of the Chiral Tagging Candidate, 3,3,3-Trifluoro-1,2-Epoxypropane and Its Complex with the Argon Atom. *J. Phys. Chem. A* **2018,** *142*, 4670-4680.

12. Marshall, M. D.; Leung, H. O. The Microwave Spectrum and Molecular Structure of 3,3-Difluoro-1,2-Epoxypropane and Its Complex with the Argon Atom. *J. Mol. Spectrosc.* **2018,** *350*, 18-26.

13. Marshall, M. D.; Leung, H. O.; Seifert, N. A.; Xu, Y.; Jäger, W. Effects of Chirality in Homodimers of 3,3,3-Trifluoro-1,2-Epoxypropane. The 73rd International Symposium on Molecular Spectroscopy, Talk TC-04, Urbana-Champaign, IL, 2018.

14. Marshall, M. D.; Leung, H. O.; Schnell, M.; Domingos, S. R.; Krin, A. The Conversion of Styrene Oxide Enantiomers into Spectroscopically Distinguishable Diastereomers through Complexation with 3,3,3-Trifluoro-1,2-Epoxypropane. The 74th International Symposium on Molecular Spectroscopy, Talk RH-02, Urbana-Champaign, IL, 2019.

15. Collins, R. A.; Legon, A. C.; Millen, D. J. Rotational Spectrum, Inversion Spectrum and Properties of the Van Der Waals Molecule Argon–Oxirane. *J. Mol. Struct. Theochem* **1986,** *135*, 435-445.

16. Moreschini, P.; Caminati, W.; Favero, P. G.; Legon, A. C. Pathways for Inversion in the Oxirane-Argon Complex. *J. Mol. Struct.* **2001,** *599*, 81-87.

17. Blanco, S.; Maris, A.; Millemaggi, A.; Caminati, W. The Most Stable Conformer of the Propylene Oxide-Argon Complex. *J. Mol. Struct.* **2002,** *612*, 309-313.

18. Blanco, S.; Melandri, S.; Maris, A.; Caminati, W.; Velino, B.; Kisiel, Z. Free Jet Rotational Spectrum of Propylene Oxide-Krypton and Modelling and *Ab Initio* Calculations for Propylene Oxide-Rare Gas Dimers. *Phys. Chem. Chem. Phys.* **2003,** *5*, 1359-1364.

19. Frisch, M. J.; Trucks, G. W.; Schlegel, H. B.; Scuseria, G. E.; Robb, M. A.; Cheeseman, J. R.; Scalmani, G.; Barone, V.; Petersson, G. A.; Nakatsuji, H., et al. *Gaussian 16*, Revision A.03; Wallingford, CT, 2016.

20. Bondi, A. Van Der Waals Volumes and Radii. *J. Phys. Chem.* **1964,** *68*, 441-451.

21. Boys, S. F.; Bernardi, F. The Calculation of Small Molecular Interactions by the Differences of Separate Total Energies. Some Procedures with Reduced Errors. *Mol. Phys.* **1970,** *19*, 553-566.

22. Marshall, F. E.; Sedo, G.; West, C.; Pate, B. H.; Allpress, S. M.; Evans, C. J.; Godfrey, P. D.; McNaughton, D.; Grubbs II, G. S. The Rotational Spectrum and Complete Heavy Atom Structure of the Chiral Molecule Verbenone. *J. Mol. Spectrosc.* **2017,** *342*, 109-115.

23. Grimme, S.; Steinmetz, M. Effects of London Dispersion Correction in Density Functional Theory on the Structures of Organic Molecules in the Gas Phase. *Phys. Chem. Chem. Phys.* **2013,** *15*, 16031-16042.

24. It is necessary to fully relax the FO geometry to perform a meaningful calculation of vibrational frequencies.

25. Marshall, M. D.; Leung, H. O.; Scheetz, B. Q.; Thaler, J. E.; Muenter, J. S. A Chirped Pulse Fourier Transform Microwave Study of the Refrigerant Alternative 2,3,3,3-Tetrafluoropropene. *J. Mol. Spectrosc.* **2011,** *266*, 37-42.

26. Marshall, M. D.; Leung, H. O.; Calvert, C. E. Molecular Structure of the Argon-(*Z*)-1-Chloro-2-Fluoroethylene Complex from Chirped-Pulse and Narrow-Band Fourier Transform Microwave Spectroscopy. *J. Mol. Spectrosc.* **2012,** *280*, 97-103.

27. Leung, H. O.; Marshall, M. D.; Messinger, J. P.; Knowlton, G. S.; Sundheim, K. M.; Cheung-Lau, J. C. The Microwave Spectra and Molecular Structures of 2-Chloro-1,1-Difluoroethylene and Its Complex with the Argon Atom. *J. Mol. Spectrosc.* **2014,** *305*, 25-33.

28. Leung, H. O.; Gangwani, D.; Grabow, J. U. Nuclear Quadrupole Hyperfine Structure in the Microwave Spectrum of Ar-N_2O. *J. Mol. Spectrosc.* **1997,** *184*, 106-112.

29. Watson, J. K. G., Aspects of Quartic and Sextic Centrifugal Effects on Rotational Energy Levels. In *Vibrational Spectra and Structure*, Durig, J. R., Ed. Elsevier Scientific Publishing: Amsterdam, 1977; Vol. 6, pp 1-89.

30. Pickett, H. M. The Fitting and Prediction of Vibration-Rotation Spectra with Spin Interactions. *J. Mol. Spectrosc.* **1991,** *148*, 371-377.

31. Kisiel, Z. Least-Squares Mass-Dependence Molecular Structures for Selected Weakly Bound Intermolecular Clusters. *J. Mol. Spectrosc.* **2003,** *218*, 58-67.

32. Kisiel, Z., Assignment and Analysis of Complex Rotational Spectra. In *Spectroscopy from Space*, Demaison, J.; Sarka, K.; Cohen, E. A., Eds. Kluwer Academic Publishers: Dordrecht, 2001.

33. Kisiel, Z. Prospe - Programs for Rotational Spectroscopy. http://info.ifpan.edu.pl/~kisiel/prospe.htm (accessed July 17, 2019).

34. Kraitchman, J. Determination of Molecular Structure from Microwave Spectroscopic Data. *Am. J. Phys.* **1953,** *21*, 17-24.

35. Imachi, M.; Kuczkowski, R. L. The Microwave Spectrum and Structure of Propylene Oxide. *J. Mol. Struct.* **1982,** *96*, 55-60.

36. Hirose, C. The Microwave Spectra and R_0, R_s, and R_m Structures of Ethylene Oxide. *Bull. Chem. Soc. Jpn.* **1974,** *47*, 1311-1318.

37. Costain, C. C. Determination of Molecular Structures from Ground State Rotational Constants. *J. Chem. Phys.* **1958,** *29*, 864-874.

TOC Graphic